Particle Dynamics in LEP at Very High Energy

F. Barbarin,* F.C. Iselin, J.M. Jowett
CERN
CH-1211 Geneva 23

Abstract

As the beam energy of LEP is increased up to 90 GeV (LEP2) and beyond, the single-particle dynamics is ever more strongly influenced by the emission of synchrotron radiation. The program MAD has recently been modified to simulate individual photon emissions in magnetic elements (or the classical component). Effects of radiation damping and quantum fluctuations (the 6-dimensional "sawtooth" closed orbit, normal modes, emittances, etc.) emerge in a completely natural way. Analysis of tracked orbits has changed the understanding of the physical effects determining the dynamic aperture of LEP2. Non-resonant radiative beta-synchrotron coupling and tune-dependences on betatron amplitudes play roles commensurate with those of the chromatic effects. Resonances and coherent excitations generate new attractors of the underlying deterministic dissipative system. Phase space distribution functions on these can be computed by including the quantum fluctuations.

1 INTRODUCTION

The energy of LEP will shortly be doubled with the addition of a large super-conducting RF system to compensate a synchrotron radiation energy loss per turn of the order of 2 % of the beam energy. This will give rise to significant "energy sawtoothing" effects which are important even at the level of closed-orbit and linear optics [1, 2]. From the values of the dimensionless parameters characterising damping and quantum excitation (see Table 1), we can say that LEP2 (like TRISTAN) will be a "very high" energy ring.

In the formulation of [3], to which we refer for details, the equations of motion of an electron or positron are

$$
\begin{aligned}
x' &= \frac{\partial H}{\partial p_x}, & p_x' &= -\frac{\partial H}{\partial x} - \frac{P_X(s)}{p_0 c^2}\frac{\partial H}{\partial p_x}, \\
y' &= \frac{\partial H}{\partial p_y}, & p_y' &= -\frac{\partial H}{\partial y} - \frac{P_X(s)}{p_0 c^2}\frac{\partial H}{\partial p_y}, \\
z_t' &= \frac{\partial H}{\partial p_t}, & p_t' &= -\frac{\partial H}{\partial z_t} + \frac{P_X(s)}{p_0 c^2}\frac{\partial H}{\partial p_t},
\end{aligned}
\tag{1}
$$

where primes denote derivatives with respect to azimuth s and $X = (x, y, z_t, p_x, p_y, \delta = (p - p_0)/p_0)$ are the particle's canonical coordinates relative to a closed reference curve[1] (all momenta are defined in units of p_0). External electromagnetic fields are described in the Hamiltonian H. The

---

*Now at LAPP, Annecy.

[1]z_t is not strictly the same as ct whose conjugate variable $p_t \equiv (E - E_0)/p_0 c \simeq \delta$ is used in MAD but the difference is numerically negligible for ultra-relativistic particles.

		LEP1	LEP2
Beam energy	E/GeV	45.6	90.0
Radiation loss	U_0/GeV	124.6	1890
Damping time	τ_x/T_0	692	90
Energy spread	$10^3\,\sigma_\varepsilon$	0.701	1.39
Quantum excitation	$10^9\,4\sigma_\varepsilon^2 T_0/\tau_x$	2.8	79
Emittance	ϵ_x/nm	12	46

Table 1: Comparison of LEP1 and LEP2 parameters for the nominal lattice with phase advances $(\mu_x, \mu_y) = (90°, 60°)$ in the arc cells; T_0 is the revolution time.

synchrotron radiation power is a stochastic function

$$
P_X(s) = c\sum_j u_j \delta(s - s_j),
\tag{2}
$$

where the s_j are the azimuthal positions where photons of energy u_j are emitted. The statistical properties of these random variables depend on the particle's momentum and the local magnetic field, i.e., on p_t, s, x and y. The closed orbit $X_0(s)$ is a 6-dimensional periodic solution of the average of (1). It includes the "stable phase" $z_{t0}(s)$ and the "energy sawtooth" $\delta_0(s)$. The horizontal component can be written as $x_0(s) = D_x(s)\delta_0(s) + x_B(s)$ where D_x is the usual dispersion and $x_B(s)$ is the Bassetti term [1]. Even in a perfect LEP at 90 GeV, $x_0(s)$ has amplitudes up to 3 mm (see [4]).

2 TRACKING FOR LEP2

2.1 Changes in MAD

Four options have been added to the tracking module of MAD [5]. Each corresponds to a different simplification of (2). In all cases involving energy loss, tracking proceeds in three steps: (1) energy loss at magnet entry, (2) tracking through the magnet, (3) energy loss at magnet exit. MAD assumes that the particle sees a constant magnetic field over each half length of the magnet; the value of the field is defined by the transverse position of the particle at the entry or exit point.

Tracking without Synchrotron Radiation ignores any energy loss due to synchrotron radiation, but includes the synchrotron motion due to RF cavities. The energy is constant on the closed orbit so the focusing functions and tunes are not correct when synchrotron radiation is important.

Symplectic Tracking around the Closed Orbit includes the systematic energy changes by radiation and

cavities to determine the closed orbit. A symplectic map is obtained around the closed orbit by making each particle lose the same energy as a particle on the closed orbit. From (1) (see also [3, 4]) the momentum changes are

$$\Delta p_{x,y} = -f_r(1+p_t)p_{x,y}, \quad \Delta p_t = -f_r(1+p_t)^2, \qquad (3)$$

where

$$f_r = \frac{2}{3}r_e \left(\frac{1+p_{t0}(s)}{mc}\right)^3 h(X_0(s),s)^2 \frac{L}{2}, \qquad (4)$$

where r_e is the classical electron radius, $h(X_0(s),s) = e|\mathbf{B}(x_0,y_0,s)|/(1+p_{t0}(s))$ is the local curvature of the *closed* orbit and $L/2$ the half-magnet length. In thin multipoles MAD uses a fictitious length for radiation to keep the curvature finite. The focusing functions, normal modes and tunes are correct with this option, but there is no radiation damping or quantum excitation. Earlier tracking studies [6] used a similar model but with the radiation loss corresponding to the *reference orbit* in dipoles only.

Tracking with Radiation Damping corresponds to the average of the stochastic terms in (1) and includes all systematic energy losses due to synchrotron radiation. This helps to find damping times and effects which may cause particle losses due to periodic energy variations. The energy loss is given by (3) and (4) except that the coordinates are those of the particle's own orbit. Thus each particle loses energy according to the fields it sees when it passes a magnet.

Tracking with Quantum Emission, the most realistic option, includes all effects of synchrotron radiation. The number N of photons to be emitted [3] in the half-magnet is sampled from the Poisson distribution with the mean

$$\overline{N} = \frac{5\sqrt{3}cr_e}{6\hbar}(1+p_{t0}(s))\, h(X_0(s),s)\frac{L}{2}. \qquad (5)$$

Then MAD samples N photon energies from the proper synchrotron radiation distribution using the algorithm specified in [3] and sums up their energies to get the energy loss to use in (3). A similar implementation in DIMAD has been used for the SLC [7].

2.2 Modelling and analysis

These and other improvements to MAD have considerably improved the modelling of the single-particle dynamics for LEP2 dynamic aperture studies. Among the features which it is now possible (and essential!) to include we mention:

- Full details of the RF cavity distribution. In this paper, all examples include each of 192 superconducting cavities around the 4 interaction points and 120 copper cavities around interaction points 2 and 6, excited with nominal voltages. However trips of cavity units have significant effects on the transverse optics.

- The vacuum chamber, modelled as a collimator in every quadrupole.

- Three-dimensional dynamic aperture scans, varying the actions of all three normal modes [4].

- Misalignments, field errors and corrections of the *average* e^+e^- *orbit*.

Auxiliary analysis software allows us to compare dynamic apertures, prepare phase space plots and spectra, fit distributions functions and identify the physical mechanisms leading to particle losses.

Most dynamic aperture studies [4] are now done with radiation damping but without the quantum fluctuations. In typical stable cases, particles are either damped to the closed orbit or lost within a few tens of turns, removing the uncertainty over the number of turns tracked which is always present in symplectic tracking.

2.3 Loss mechanisms

General nonlinear motion at large amplitudes in 6 dimensions is difficult to describe briefly. However in special
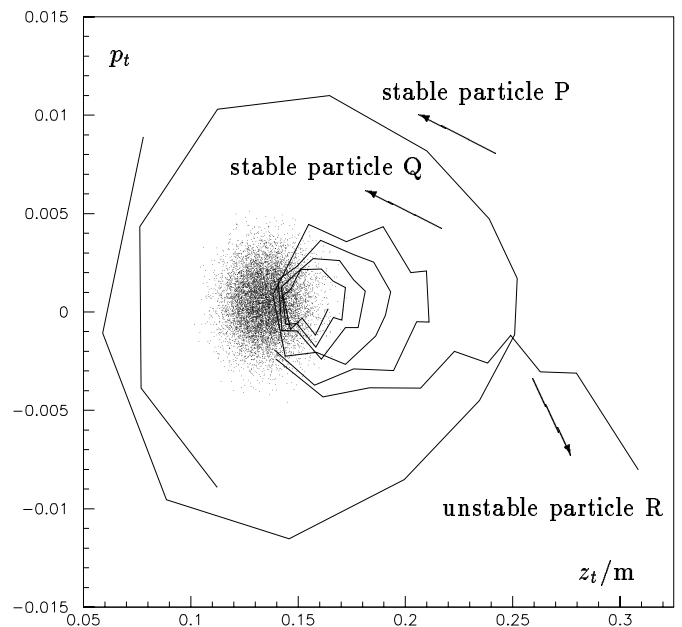

Figure 1: The vertical Radiative Beta-synchrotron Coupling Instability in LEP at 90 GeV, projected into synchrotron phase space. The continuous lines show the motion of three particles P, Q and R, tracked with damping. P starts off with large (z_t, p_t) but zero betatron amplitudes. It remains stable and starts to damp to the stable phase. Q and R start with $y = 5.5$ mm and 6 mm, and initial (z_t, p_t) on the closed orbit. Q can be loosely described as executing synchrotron oscillations about a shifted stable phase angle which adiabatically damps to the closed orbit. R's amplitude grows in a few turns until it is lost. A fourth particle has been tracked with quantum emission (for 10^4 turns) to give the cloud of points representing the core of the beam around the closed orbit.
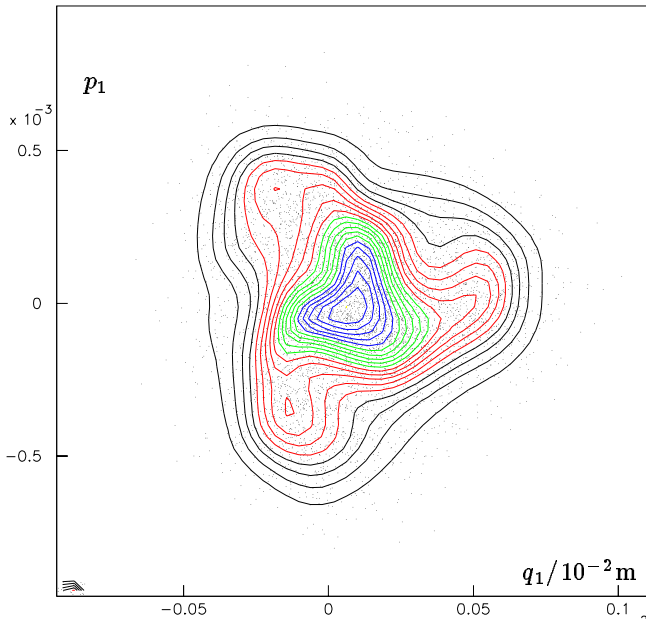
Figure 2: Smoothed and fitted distribution in horizontal betatron phase space $(q_1, p_1) \simeq (x_\beta, p_{x\beta})$ around the closed orbit and the period 3 fixed points of a third-order resonance in a low-emittance lattice adjusted to $Q_x = 125.35$ One particle has been tracked with quantum emission (for 10^4 turns).
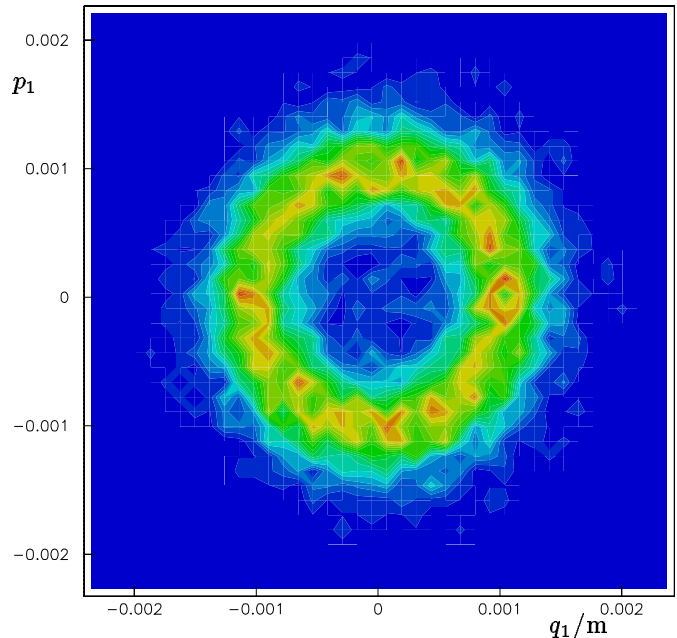

Figure 3: Distribution (lighter tones represent higher density) in horizontal betatron phase space around the limit cycle generated by a coherent excitation of the beam with a kicker exciting close to the tune. One particle has been tracked with quantum emission (for 10^4 turns). Additional resonance islands and small attracting structures are visible.

cases one can identify and name an instability mechanism. The familiar chromatic effects, resonances, synchro-betatron couplings and, notably, tune-dependences on betatron amplitude remain important at LEP2 but new loss mechanisms arise from the strong radiation. One such is illustrated in Figure 1. Here the extra radiation loss in quadrupoles due to large *transverse* amplitudes drives the particle unstable in *synchrotron* phase space. This is an important hard limit on transverse dynamic aperture [4] and can only be seen when damping is included.

2.4 Phase Space Distributions

Phase space distribution functions can be computed by tracking with quantum fluctuations for a large number of turns. Generally, an attractive fixed point or period n cycle of the underlying dissipative map will give rise to n local maximums of the distribution function. Their heights are related to the measure of the basin of attraction of the fixed point. When resonances are not important, a single fixed point on the closed orbit is visible and we recover the familiar gaussian distributions with the proper emittances.

Figure 2 shows a more interesting example for a LEP2 lattice working close to the resonance $3Q_1 = 376$.

Other topologies for the attractors of a dissipative system are possible. Figure 3 shows the case where a coherent excitation by a kicker exciting the beam close to the horizontal betatron tune Q_1 generates a limit cycle of the dissipative system, resulting in a crater-like distribution with further fine structure just inside its lip.

3   CONCLUSIONS

A representation of the radiation effects in e^+e^- rings has been incorporated in MAD. It is *faithful in detail* so that all physical phenomena, such as damping times and emittances, arise completely naturally from the optics and RF parameters. We have used it to show that the physical effects determining the dynamic aperture at LEP2 are quite different from those in rings where radiation is less important. While some well-known effects diminish in importance, radiation damping itself can create new instability mechanisms. Non-gaussian phase space distribution functions can also be calculated.

4   REFERENCES

[1] M. Bassetti, Proc. 11th International Conference on High-energy accelerators, Birkhäuser, Basel, (1980) 650.

[2] M. Kikuchi, Nucl. Instr. and Methods, **A301** (1991) 37.

[3] J.M. Jowett, AIP Conference Proceedings 153 (1987) 864.

[4] J.M. Jowett in Proc. 4th Workshop on LEP Performance, CERN SL/94-06 (1994) 47.

[5] H. Grote, F.C. Iselin, CERN SL 90–13 (AP) rev. 3 (1993).

[6] F. Ruggiero, Proc. 1989 Particle Accelerator Conf., 1298.

[7] G. Roy, Nucl. Instr. and Methods, **A298** (1990) 128.